Comparison of dissociative ionization of H_2, N_2, Ar_2, and CO by elliptically polarized two-color pulses

J. Wu,[1,2] A. Vredenborg,[2] L. Ph. H. Schmidt,[2] T. Jahnke,[2] A. Czasch,[2] and R. Dörner[2,*]

[1]*State Key Laboratory of Precision Spectroscopy, East China Normal University, Shanghai 200062, China*

[2]*Institut für Kernphysik, Goethe Universität, Max-von-Laue-Strasse 1, D-60438 Frankfurt, Germany*

(Received 11 November 2012; published 13 February 2013)

We study the directional dissociative ionization of diatomic molecules (H_2, N_2, Ar_2, and CO) by intense phase-controlled elliptically polarized two-color pulses. The phase between the two colors of our elliptically polarized two-color pulse is unambiguously and straightforwardly assigned by tracing the momentum of the released electron, streaked by the rotating laser field, which is imprinted in the momentum of the correlated ion. The laser-driven electron motion, electron-localization-assisted enhanced multielectron ionization, and role of the orbital shape for the asymmetric dissociative ionizations of various molecules are discussed.

DOI: 10.1103/PhysRevA.87.023406 PACS number(s): 33.80.Rv, 33.80.Gj, 42.50.Hz, 42.65.Re

I. INTRODUCTION

As a primary and significant step in understanding and manipulating molecular reactions, the breaking of chemical bonds, e.g., dissociative ionization of molecules, in precisely controlled laser fields has attracted much attention. An asymmetric laser field of few-cycle [1–3] or two-color pulses [4–9] was demonstrated to be a powerful tool to steer chemical bond breaking, leading to directional ejection of ionic fragments. However, most of the studies of phase-dependent asymmetric dissociative ionization of molecules were performed by using linearly polarized ultrashort laser pulses, which suffer from complexity of the phase calibration and the involved recollision process of the tunneled electron.

Instead of linear polarization, in this paper, we use phase-controlled elliptically polarized two-color pulses to study the phase-dependent directional dissociative ionization of molecules. The phase between the two colors of an elliptically polarized two-color pulse is straightforwardly determined by tracing the momentum vector of the released electron, which is streaked by the rotating laser field in our measurement. The elliptical field also suppresses recollisions. The lightest molecule H_2, the tightly bound homonuclear molecule N_2, the heteronuclear molecule CO, and the van der Waals–bound rare-gas dimer Ar_2 were studied. The ion-energy-dependent directional ejection of a proton was observed in single-electron dissociative ionization of H_2 due to the laser-driven motion of the bound electron during the dissociation of the molecular ion or the phase-dependent interference of various dissociation pathways. The asymmetric multielectron dissociative ionization of N_2 and Ar_2 was found to be consistent with the classical picture of electron-localization-assisted enhanced ionization [10], i.e., the electron localized in the up-field potential well of the molecular ion is much favored to be freed rather than the down-field one. The multielectron dissociative ionization of CO was dominated by the profiles of the ionizing molecular orbitals.

One of the most important aspects of this study is to assign the laboratory-frame direction of the maximum of the asymmetric laser field for each ionization event. This direction is given by the relative phase ϕ between the fundamental-wave (FW) and second-harmonic (SH) components of the two-color pulse. For the case of linear polarization this phase can be obtained *in situ* only from the electrons in the high-energy region of the electron spectrum. These fast electrons are accelerated to their final energy by rescattering at the ionic core during the pulse. The details of the rescattering process are highly sensitive to the phase between the two colors [11]. Therefore, as shown in Refs. [10,11], the phase can be retrieved only if the backscattered electrons are unambiguously identified within the whole spectrum. Since the maximum energy of a rescattering electron does not always occur at $\phi = 0$ or π, the measured profile of the phase-energy-dependent electron spectrum has to be compared with a numerical simulation which also varies for different targets.

II. EXPERIMENTAL SETUP AND LASER PHASE CALIBRATION

We overcome this complexity of the crucial phase assignment by taking advantage of the angular streaking [12–17] due to the elliptically polarized two-color pulse. The rotating laser field greatly suppresses the recollision of the freed electron [15,18] and the direction of its final momentum vector is readily locked to the phase of the laser field, i.e., perpendicular to the field direction at the instant of ionization [12–17]. Experimentally, we produce the elliptically polarized two-color pulse with variable phase in a collinear scheme as shown in Fig. 1(a). Briefly, a femtosecond laser pulse (35 fs, 790 nm) was frequency doubled using type-I phase matching in a 200-μm-thick β-barium borate (BBO) crystal. The polarization of the FW was then rotated to be parallel to that of the SH (along the y axis in our experiment) by using a dual-wavelength plate. The time lag between them was finely tuned with a birefringent α-BBO crystal. We then changed the polarization of the two-color pulse from linear to elliptical by using a quarter-wave plate centered at the SH wavelength. A pair of fused silica wedges was used to continuously vary the phase ϕ of the two-color pulse which is directly imprinted in the momenta of the freed electrons or the correlated ions.

*doerner@atom.uni-frankfurt.de

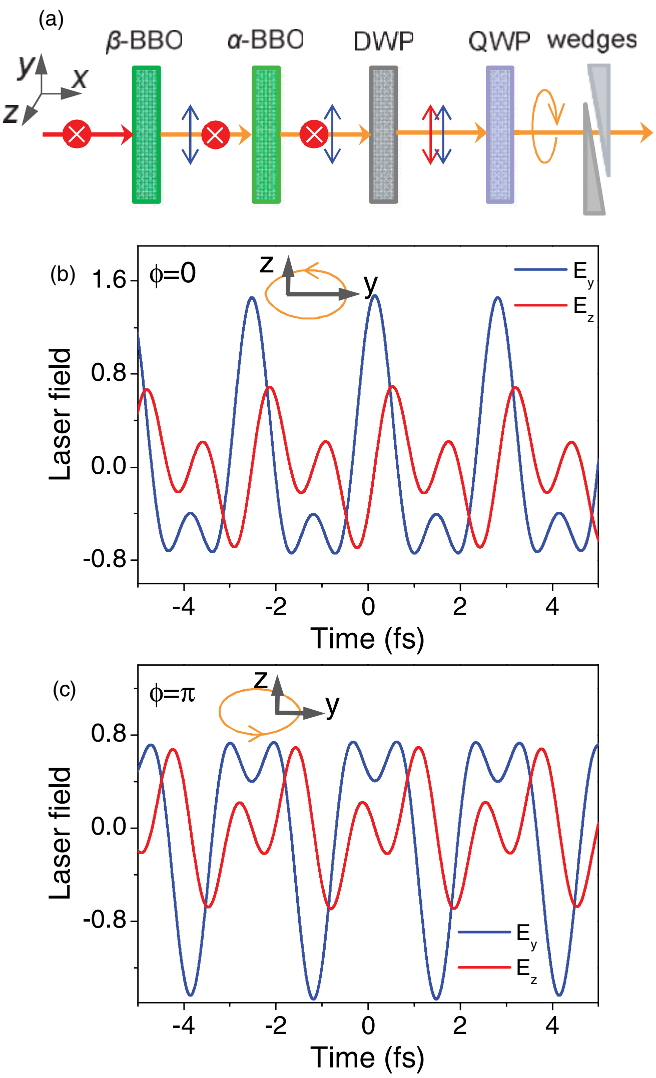

FIG. 1. (Color online) (a) Scheme of collinear generation of two-color laser pulse. DWP, dual-wavelength wave plate; QWP, quarter-wave plate. (b),(c) Time-dependent oscillations of the electric fields along y (blue, light gray in black-and-white print) and z (red, dark gray in black-and-white print) axes of the elliptically polarized two-color pulse at (b) $\phi = 0$ and (c) $\phi = \pi$, respectively. The inset ellipses show the counterclockwise rotating sense of the elliptically polarized pulse.

Figure 1(b) shows the electric fields of our elliptically polarized two-color pulse at $\phi = 0$; the major and minor axes are oriented along the y and z axes [the inset (orange) ellipse], respectively. The tunneling ionization probability is maximized when the laser field points in the $+y$ direction since it steeply depends on the field strength, which results in a concentration of counts along $-z$, i.e., $pz_e < 0$, due to the streaking by the counterclockwise rotating laser field [19]. For $\phi = \pi$ [Fig. 1(c)], the maximal laser field of the two-color pulse alters to the $-y$ direction, which correspondingly changes the maximum in the electron momentum distribution to $+z$, i.e., $pz_e > 0$. Therefore, by analyzing the asymmetry of the electron momentum distribution along the z axis (pz_e), we can straightforwardly trace the phase ϕ of the elliptically polarized two-color pulse. Technically, instead of directly detecting the electron, we measured the momentum of the correlated ion

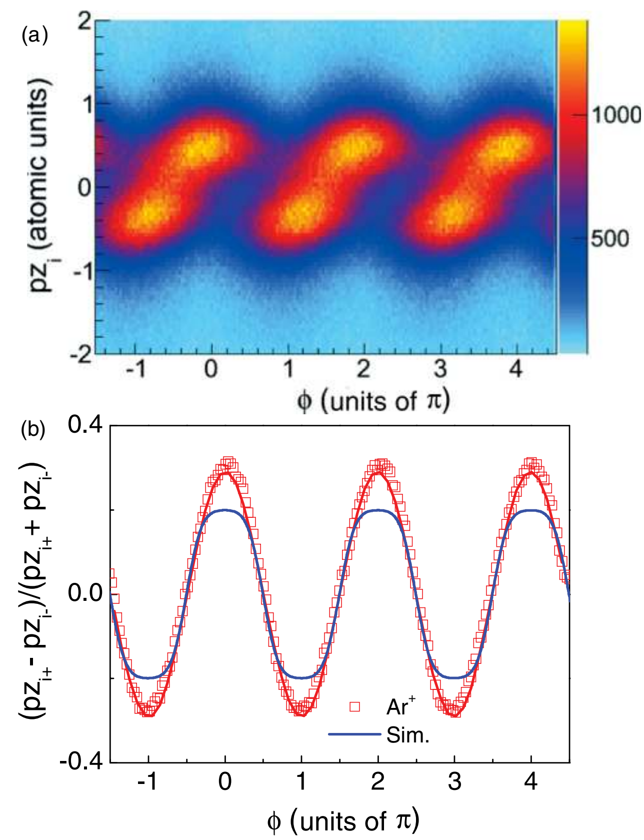

FIG. 2. (Color online) Phase calibration via single ionization of atomic Ar. (a) Phase-dependent distribution of the momentum of Ar^+ along the z axis (b) Phase-dependent directional ejection of Ar^+ as the recoil of the released electron (red curve with squares). (The blue solid curve shows the classically simulated result, which agrees well with the experimental measurement.

which is the recoil of the released electron. This further simplifies the phase tracing, which is meanwhile insensitive to the target. We performed the measurements in a standard reaction microscope of cold-target recoil-ion momentum spectroscopy (COLTRIMS) [20,21]. The elliptically polarized two-color pulse was tightly focused onto a supersonic gas jet by a concave mirror ($f = 7.5$ cm). The gas jet was a mixture of Ar (89 %), N_2 (10 %), and CO (1 %), so various molecules were measured under the same conditions. H_2 is the main contribution to the residual background gas for the ultrahigh vacuum surroundings ($<10^{-10}$ mbar) in our experiment, which was hence directly used for the study of dissociative ionization of H_2. The ionization-induced ion fragments were detected by a time- and position-sensitive detector [22] at the end of the spectrometer after acceleration by a weak static and homogeneous electric field. The intensities of the SH and FW components inside the two-color pulse were estimated to be 3.4×10^{14} and 7.6×10^{14} W/cm^2, respectively.

Figure 2(a) shows the measured ion momentum of Ar^+ from single ionization of atomic Ar ($Ar \rightarrow Ar^+ + e$) along the z axis ($pz_i = -pz_e$) versus the phase of our elliptically polarized two-color pulse. As the ion momentum is the recoil momentum of the released electron, $pz_i > 0$ and $pz_i < 0$ correspond to the laser phases $\phi = 0$ and $\phi = \pi$, respectively. To intuitively illustrate this, we compare the ejection probabilities of Ar^+ to $+z$ (pz_{i+}) and $-z$ (pz_{i-}), i.e., $(pz_{i+} - pz_{i-})/(pz_{i+} + pz_{i-})$, [Fig. 2(b) (red squares)], for which the positive and negative maxima occur for $\phi = \pm 2n\pi$ and $\phi = (\pm 2n + 1)\pi$, respectively. The classical motion and the resulting final momentum of the released electron in our elliptically polarized two-color pulse of various phases were calculated; the Ammosov-Delone-Krainov (ADK) rate [23] was taken as a weight for each trajectory. The initial momentum at the instant of ionization was assumed to be zero. The blue solid curve in Fig. 2(b) shows the simulated phase-dependent asymmetric ejection of the correlated ion along the z axis, which agrees well with the experimental measurement. For the field intensities in our experiment, the ADK rate of single ionization of Ar is partially saturated [24]. This crudeness of the ADK model for our conditions, however, does not affect the phase-dependent asymmetric ejection of Ar^+, as we numerically tested by decreasing the field intensity to 1.0×10^{14} W/cm^2, which primarily reduces the magnitude of the streaking momentum. Our laser phase assignment for the elliptically polarized two-color pulse is realized in the same measurement as all the molecular ionization channels that we interest in. It therefore avoids possible errors due to subsequent measurements.

III. H_2

We first discuss the directional dissociative ionization of H_2, the simplest and lightest diatomic molecule, which has been well studied by using linearly polarized few-cycle or two-color pulses in Refs. [2,5]. Following the release of one electron, the molecular ion $H_2{}^+$ starts to dissociate in the laser field. The oscillating laser field subsequently drives the forth-and-back motion of the remaining bound electron between the nuclei, which is finally localized at one of the protons when the potential barrier between them is higher than the driving energy of the laser field. This results in phase-dependent directional ejection of the proton [1–7]. Alternatively, it can be understood to be the phase-dependent interference of various dissociation channels. These two pictures actually give the same result, i.e., the directional dissociative ionization of H_2 depends on the energy of the ejected proton and the phase of the driving laser field.

Figure 3(a) shows the measured kinetic-energy release (KER) of $H_2 \rightarrow H^+ + H + e$, which we will refer to as the $H_2(1,0)$ dissociative ionization channel. It divides into low-KER (less than 0.6 eV) and high-KER (greater than 0.6 eV) dissociation regions. As shown in the inset of Fig. 3(b), starting from the single-electron ionization nuclear wave packet of $H_2{}^+$ launching on the g (gerade) potential energy surface, there are two possible pathways to reach the low-KER dissociation region [7]: The nuclear wave packet transits to the u (ungerade) state from the g state by absorbing one FW photon and then directly dissociates through the u curve; alternatively, it can first transit to the u state by absorbing one SH photon, later couple back to the g state by emitting one FW photon, and then dissociate through the g curve. The measured signal strength resulting from the interference of these two pathways is governed by the accumulated phases of the nuclear wave packets during their dissociation, which is directly locked to the phase ϕ of the two-color pulse. Therefore, as

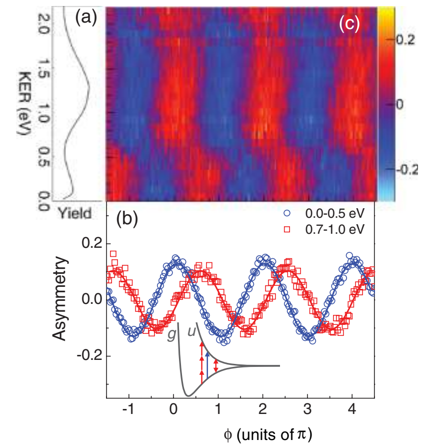

FIG. 3. (Color online) (a) KER of $H_2(1,0)$ channel integrated over all the laser phases. (b) Asymmetries integrated over $0 - 0.5$ eV (blue circles, low KER) and $0.7 - 1.0$ eV (red squares, high KER) regions. The solid curves are the fits of the measured data. The inset schematically shows the involved transitions of the dissociating nuclear wave packet between the g and u states of $H_2{}^+$. The blue (light gray in black-and-white print) and red (dark gray in black-and-white print) arrows stand for the FW and SH photons, respectively. (c) Energy-phase-dependent asymmetric ejection of H^+ from $H_2(1,0)$.

shown in Fig. 3(c), the ejection direction of H^+ oscillates as a function of the laser phase. We define an asymmetry parameter of $\beta = (P_{y+} - P_{y-})/(P_{y+} + P_{y-})$, where P_{y+} and P_{y-} stand for the probabilities of H^+ being emitted to $+y$ and $-y$, respectively. Similarly, as shown in Fig. 3(c), clear phase-dependent directional ejection of H^+ is observed for the high-KER region. It can be understood to be the phase-dependent interference of the following two pathways: The nuclear wave packet launched in the g state transits to the u state by absorbing one SH photon and then directly dissociates through the u curve; or, alternatively, it can first transit to the u state by absorbing three FW photons, later transit back to the g state by emitting one FW photon, and then dissociate through the g curve. The different phase dependences of the low- and high-KER regions are due to the different dissociation times and various laser phases experienced by the nuclear wave packets at the instants of transitions between the g and u states. Figure 3(b) shows the asymmetries of the $H_2(1,0)$ channel integrated for the low- and high-KER regions, which are shifted by $\sim 0.5\pi$ from each other.

IV. N_2 AND Ar_2

For N_2, we focus on the asymmetric double- [$N_2 \rightarrow N^{2+} + N + 2e$, denoted as $N_2(2,0)$] and triple- [$N_2 \rightarrow N^{2+} + N^+ + 3e$, denoted as $N_2(2,1)$] ionization channels. Experimentally the $N_2(2,1)$ channel can be directly identified in our coincidence and here we study its directional dissociative ionization with respect to the Coulomb potential effect of the molecular ion on the tunneling electron [19]. For $N_2(2,0)$ we do not detect the neutral species, but we can clearly separate it from the $N_2(2,1)$ events by the much lower KER [see the inset of Fig. 4(a)]. Remarkably the N^{2+} direction is different for the $N_2(2,0)$ and $N_2(2,1)$ channels [Fig. 4(a)]. This directly shows that the $N_2(2,1)$ channel is not produced by

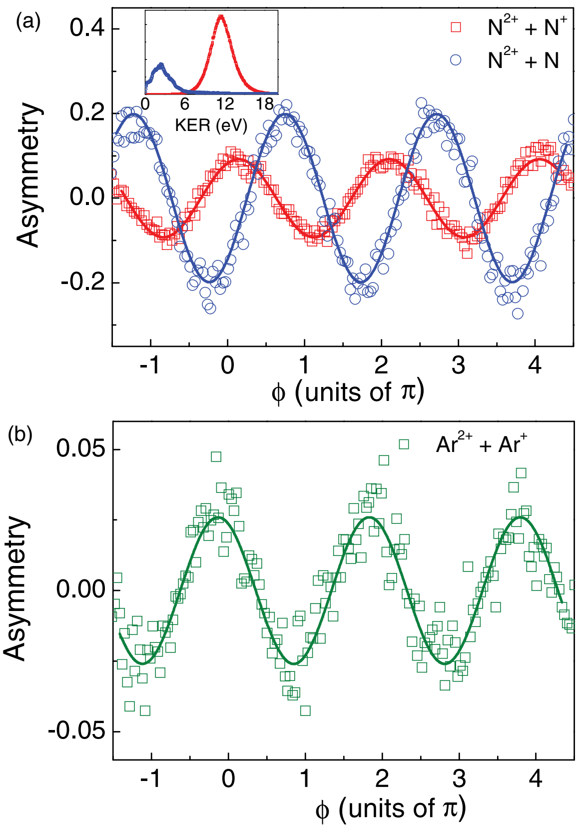

FIG. 4. (Color online) (a) Phase-dependent asymmetries of the directional ejection of N^{2+} from the $N_2(2,0)$ (blue circles) and $N_2(2,1)$ (red squares) channels. The corresponding KERs are shown in the inset. (b) Phase-dependent asymmetry of the directional ejection of Ar^{2+} from $Ar_2(2,1)$. The solid curves are the numerical fits of the measured data.

sequential ionization of the intermediate $N_2(2,0)$. $N_2(2,1)$ is hence produced through the intermediate $N_2(1,1)$, i.e., $N_2 \rightarrow N^+ + N^+ + 2e$. This conclusion is supported by Fig. 4(a) which shows that the N^{2+} from $N_2(2,1)$ is created on the side of the molecule which was uphill in the potential. This is in agreement with the expectation from the electron-localization-assisted enhanced ionization [8,9,25–29]. The third electron will preferably escape from the up-field core where it needs to tunnel only through the narrow inner barrier.

We find the same directionality as for the $N_2(2,1)$ also for the directional dissociative multielectron ionization of the van der Waals–bound rare-gas dimer Ar_2, as shown in Fig. 4(b) for $Ar_2 \rightarrow Ar^{2+} + Ar^+ + 3e$, indicating the universality of the classical picture of the enhanced multielectron ionization of molecules [9].

V. CO

We finally discuss our results for CO as an example of a heteronuclear diatomic molecule. The reason for asymmetries in this case is completely different from the cases of homonuclear species. In CO, the ionizing orbital itself is asymmetric. As recently demonstrated [10,17], it is this asymmetry of the molecular orbital which creates the directional dissociation of CO. The first electron from CO is more likely to be freed when the laser field points from C to O. This is also the case for the release of the second electron, as demonstrated in Ref. [17] by using elliptically polarized single-color pulses. These previous findings are further confirmed by our present data with phase-controlled elliptically polarized two-color pulses as shown in Fig. 5(a) for the dissociative double-ionization channel CO(1,1), i.e., $CO_2 \rightarrow C^+ + O^+ + 2e$. Starting from CO^{2+}, the third electron can be freed when the laser field points either from C to O or from O to C. Figure 5(b) shows the phase-dependent dissociative triple-ionization channels of CO(1,2), i.e., $CO_2 \rightarrow C^+ + O^{2+} + 3e$, and CO(2,1), i.e**.**, $CO_2 \rightarrow C^{2+} + O^+ + 3e$. Both show similar phase dependence as CO(1,1), indicating the dominating role of the profiles of the ionizing orbitals. Here, for the dissociative ionization of CO, the asymmetries are calculated for the emission direction of carbon ions, i.e., C^+ for CO(1,1) and CO(1,2) and C^{2+} for CO(2,1). The multielectron enhanced ionization and the profile of the molecular orbital collaborate to produce the directional dissociation of CO(1,2); it hence shows a larger asymmetry as compared to that of CO(2,1) where these two effects play opposite roles on the directional release of the third electron.

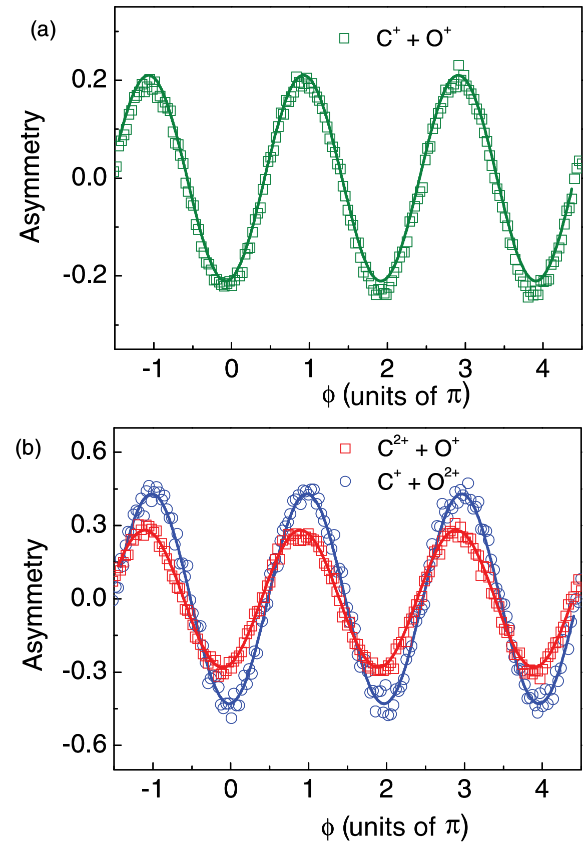

FIG. 5. (Color online) Phase-dependent asymmetries of the directional ejection of (a) C^+ from CO(1,1), (b) C^+ from CO(1,2), and C^{2+} from CO(2,1). The solid curves are the numerical fits of the measured data.

VI. CONCLUSIONS

In summary, by using elliptically polarized two-color pulses, we observed a strong phase-dependent directional dissociative ionization of H_2, N_2, Ar_2, and CO, which is governed by the laser-field-driven electron motion [1–7], electron-localization-assisted enhanced multielectron ionization [8,9,25–29], and the profiles of the ionizing orbitals [10,17], respectively. With respect to linear polarization, our elliptically polarized two-color pulse suppresses the recollision mechanism and provides a straightforward and robust approach to unambiguous assignment of the absolute laser phase by tracing the rotating-field-streaked momentum of the released electron or its recoil on the correlated ion.

ACKNOWLEDGMENTS

We acknowledge stimulating discussions with R. R. Jones and A. Becker. The work was supported by a Koselleck Project of the Deutsche Forschungsgemeinschaft. J.W. acknowledges support by the Alexander von Humboldt Foundation, the Program for New Century Excellent Talents in University (Grant No. NCET-12-0177), and the Program for Professor of Special Appointment (Eastern Scholar) at Shanghai Institutions of Higher Learning.

[1] M. F. Kling, Ch. Siedschlag, A. J. Verhoef, J. I. Khan, M. Schultze, Th. Uphues, Y. Ni, M. Uiberacker, M. Drescher, F. Krausz, and M. J. J. Vrakking, Science **312**, 246 (2006).
[2] M. Kremer, B. Fischer, B. Feuerstein, V. L. B. de Jesus, V. Sharma, C. Hofrichter, A. Rudenko, U. Thumm, C. D. Schröter, R. Moshammer, and J. Ullrich, Phys. Rev. Lett. **103**, 213003 (2009).
[3] I. Znakovskaya, P. von den Hoff, G. Marcus, S. Zherebtsov, B. Bergues, X. Gu, Y. Deng, M. J. J. Vrakking, R. Kienberger, F. Krausz, R. de Vivie-Riedle, and M. F. Kling, Phys. Rev. Lett. **108**, 063002 (2012).
[4] B. Sheehy, B. Walker, and L. F. DiMauro, Phys. Rev. Lett. **74**, 4799 (1995).
[5] M. R. Thompson, M. K. Thomas, P. F. Taday, J. H. Posthumus, A. J. Langley, L. J. Frasinski, and K. Codling, J. Phys. B **30**, 5755 (1997).
[6] H. Ohmura, N. Saito, and M. Tachiya, Phys. Rev. Lett. **96**, 173001 (2006).
[7] D. Ray, F. He, S. De, W. Cao, H. Mashiko, P. Ranitovic, K. P. Singh, I. Znakovskaya, U. Thumm, G. G. Paulus, M. F. Kling, I. V. Litvinyuk, and C. L. Cocke, Phys. Rev. Lett. **103**, 223201 (2009).
[8] K. J. Betsch, D. W. Pinkham, and R. R. Jones, Phys. Rev. Lett. **105**, 223002 (2010).
[9] J. Wu, M. Meckel, L. Ph. H. Schmidt, M. Kunitski, S. Voss, H. Sann, H. Kim, T. Jahnke, A. Czasch, and R. Dörner, Nat. Commun. **3**, 1113 (2012).
[10] H. Li, D. Ray, S. De, I. Znakovskaya, W. Cao, G. Laurent, Z. Wang, M. F. Kling, A. T. Le, and C. L. Cocke, Phys. Rev. A **84**, 043429 (2011).
[11] D. Ray, Z. Chen, S. De, W. Cao, I. V. Litvinyuk, A. T. Le, C. D. Lin, M. F. Kling, and C. L. Cocke, Phys. Rev. A **83**, 013410 (2011).
[12] P. Eckle, M. Smolarski, P. Schlup, J. Biegert, A. Staudte, M. Schöffler, H. G. Muller, R. Dörner, and U. Keller, Nat. Phys. **4**, 565 (2008).
[13] P. Eckle, A. Pfeiffer, C. Cirelli, A. Staudte, R. Dörner, H. G. Muller, M. Büttiker, and U. Keller, Science **322**, 1525 (2008).
[14] L. Holmegaard, J. L. Hansen, L. Kalhøj, S. L. Kragh, H. Stapelfeldt, F. Filsinger, J. Küpper, G. Meijer, D. Dimitrovski, M. Abu-samha, C. P. J. Martiny, and L. Bojer Madsen, Nat. Phys. **6**, 428 (2010).
[15] A. N. Pfeiffer, C. Cirelli, M. Smolarski, R. Dörner, and U. Keller, Nat. Phys. **7**, 428 (2011).
[16] X. Zhu, Q. Zhang, W. Hong, P. Lu, and Z. Xu, Opt. Express **19**, 13722 (2011).
[17] J. Wu, L. P. H. Schmidt, M. Kunitski, M. Meckel, S. Voss, H. Sann, H. Kim, T. Jahnke, A. Czasch, and R. Dörner, Phys. Rev. Lett. **108**, 183001 (2012).
[18] P. B. Corkum, Phys. Rev. Lett. **71**, 1994 (1993).
[19] J. Wu, M. Meckel, S. Voss, H. Sann, M. Kunitski, L. P. H. Schmidt, A. Czasch, H. Kim, T. Jahnke, and R. Dörner, Phys. Rev. Lett. **108**, 043002 (2012).
[20] J. Ullrich, R. Moshammer, R. Dörner, O. Jagutzki, V. Mergel, H. Schmidt-Böcking, and L. Spielberger, J. Phys. B **30**, 2917 (1997).
[21] R. Dörner, V. Mergel, O. Jagutzki, L. Spielberger, J. Ullrich, R. Moshammer, and H. Schmidt-Böcking, Phys. Rep. **330**, 95 (2000).
[22] O. Jagutzki, V. Mergel, K. Ullmann-Pfleger, L. Spielberger, U. Spillmann, R. Dörner, and H. Schmidt-Böcking, Nucl. Instrum. Methods Phys. Res., Sect. A **477**, 244 (2002).
[23] X. M. Tong, Z. X. Zhao, and C. D. Lin, Phys. Rev. A **66**, 033402 (2002), and references therein..
[24] C. Guo, M. Li, J. P. Nibarger, and G. N. Gibson, Phys. Rev. A **58**, R4271 (1998).
[25] E. Constant, H. Stapelfeldt, and P. B. Corkum, Phys. Rev. Lett. **76**, 4140 (1996).
[26] K. Codling, L. J. Frasinski, and P. A. Hatherly, J. Phys. B **22**, L321 (1989).
[27] T. Seideman, M. Yu. Ivanov, and P. B. Corkum, Phys. Rev. Lett. **75**, 2819 (1995).
[28] T. Zuo and A. D. Bandrauk, Phys. Rev. A **52**, R2511 (1995).
[29] S. Chelkowski and A. D. Bandrauk, J. Phys. B **28**, L723 (1995).